Molecular dynamics simulations of freezing of water and salt solutions

*Luboš Vrbka and Pavel Jungwirth**

Institute of Organic Chemistry and Biochemistry, Academy of Sciences of the Czech Republic, and Center for Biomolecules and Complex Molecular Systems, Flemingovo nám. 2, 16610 Prague 6, Czech Republic

Abstract

Results of extensive molecular dynamics simulations of freezing of neat water and aqueous sodium chloride solutions are reported. The process of water freezing in contact with an ice patch is analysed at a molecular level and a robust simulation protocol within the employed force field is established. Upon addition of a small amount of NaCl brine rejection from the freezing salt solution is observed and the anti-freeze effect of the added salt is described.

**Corresponding author E-mail: pavel.jungwirth@uochb.cas.cz*

I. Introduction

Water freezing is a ubiquitous natural seasonal phenomenon in mid-lattitudes, which is also daily encountered in refrigeration processes. Nevertheless, modeling studies of water freezing with atomistic resolution are relatively new and rare. This is due to the fact that molecular simulations of crystallizations in general are considered to be difficult, primarily due to complicated potential energy landscapes and long time scales involved.[1-3] As a matter of fact, we are aware of only a single successful molecular dynamics (MD) simulation of freezing of water from scratch.[1] In this extremely long simulation an ice nucleus was eventually formed spontaneously and, consequently, the whole system froze.

In order to facilitate the simulations of the freezing process, several researchers proceeded by putting a box of water in direct contact with a pre-built ice patch.[4-15] Doing this one gives up on simulating the rare event of the spontaneous formation of an ice nucleus, which is the first step for homogeneous ice freezing. One gains, however, immensely in computational efficiency, being still able to study ice growths and ice/water coexistence. In general, MD simulations with simple water potentials, such as the SPC/E model,[16] describe the aqueous liquid and ice phases quite realistically, except that they tend to give too low melting points.[17] A recent, 6-site water model, specifically developed for water/ice simulations provides a significant improvement in this respect.[11,18]

Most recently, we have extended the above simulation approach to modeling of brine rejection from freezing salt solutions.[19] This Letter has reported on first molecular simulation which shows expulsion of aqueous salt ions by the proceeding freezing front. Brine rejection is a direct demonstration of the immense disparity in salt solubilities in water (molar values) and ice (micromolar at best). Indeed, above the eutectic point of a given salt (e.g., -21.1 °C for NaCl) the solution freezes as pure

ice and salt ions are expelled into the unfrozen part of the system. This effect has important climatic conseqences during ocean freezing at high lattitudes,[20,21] and it has been also invoked in impact droplet freezing in the process of thundercloud electrification.[22] The present study represents a major extension of our previous work, which provides a detailed account on a series of new MD similations of freezing of neat water and salt solutions in contact with a patch of ice. With a sufficient amount of simulation data and after a detailed analysis in terms of time-dependent density profiles and hydrogen bonding we can extract general patterns of the freezing behavior within the present force field.

II. Computational methodology and simulation setup

Classical equations of motion for the sub-microsecond production MD runs were solved numerically with the timestep of 1 fs. Peridic boundary conditions with prismatic unit cells of different sizes were employed (see below). For each unit cell, a cutoff distance for van der Waals and Coulomb interactions was chosen close to one half of the smallest size of the unit cell. A smooth particle mesh Ewald procedure[23] was used to account for the long-range electrostatic interactions. All oxygen-hydrogen bonds were constrained by the SHAKE algorithm.[24] Temperature was kept at a desired value using the Berendsen coupling scheme.[25] For constant pressure simulations, the pressure was held at 1 atm. Use of an anisotropic pressure coupling was necessary due to the inherent anisotropy present in the initial ice/water layered structures. Note, however, that this anisotropy is relatively weak compared to the large pressure fluctuations in water. All simulations were carried out using the PMEMD program (version 3.1),[26] which is based on the AMBER 7 software package.[27] Water molecules wee described by the rigid SPC/E potential,[16] while the potential parametres the Na^+ and Cl^- were taken as the non-polarizable version from

Ref. [28].

For the construction of the simulation cell we followed the procedure outlined by Hayward and Haymet.[7] A unit cell of the shape of a rectangular prism of proton disordered cubic ice[29] with zero overall dipole moment was equilibrated at 200 K. The same unit cell was then melted and equilibrated at 300 K. One such solid and one or sevaral such liquid "building blocks" were then put together to create the desired ice(111)/water interfaces, and three-dimensional periodic boundary conditions were applied. Several simulation cells of different sizes were prepared this way. The detailed properties of all these unit cells are summarized in Table 1. Simulation cells containing salt water were prepared using the two cells presented at the bottom of Table 1 by replacing randomly chosen liquid phase water molecules by an appropriate number of sodium and chloride ions, as described in detail in Table 2.

To equilibrate the ice/water interface, we again adapted for our purpose the procedure described in detail by Hayward and Haymet.[7] Positions of ice phase water molecules were kept fixed during the equilibraion process. Several consecutive constant volume runs with different timesteps ranging from 0.1 to 1.0 fs and temperature fixed at 300 K were used to remove potential bad contacts introduced during the simulation cell construction. 50 ps constant volume simulations, followed by 100 ps constant pressure runs were used to provide relaxed systems. Finally, velocities of the solid phase water molecules were assigned their original values.

Long, sub-microsecond production runs then followed with all water molecules moving freely. Vega et al. recently reported estimates of melting points of several widely used water models.[17] Based on these results, the temperature in the simulations was constrained at different values ranging from -15° to +15° from 215 K, which is the estimated the melting point of the SPC/E water model.[17] In the following text, this melting point is assigned the relative value of 0°.

The resulting trajectories were analyzed in terms of density profiles. The simulation box was divided into 0.2 Å thick slices parallel to the interface and distributions of oxygen atoms and both ions were recorded. Figure 1 displays the simulation cell of the system *box180* (Table 1) together with the oxygen density profile. Note the characteristic repeating double-peak pattern of the density plot in the left part of the figure corresponding to the ice bilayers, while the liquid region of the simulation cell is characterized by a uniform oxygen density.

Cubic ice, which has very similar properties to the most commmon hexagonal ice (of which it is a metastable form) was chosen as a freezing template in the present simulations. One of the reasons of this choice is that cubic ice was found recently as the phase being predomoninantly formed during freezing of water droplets with radii up to 15 nm or water films up to 10 nm,[30] which are comparable in thickness to the present ice patches. Freezing to cubic ice was reported for water confined in nanopores, too.[31] Moreover, this type of ice is also present in the upper atmosphere and can play an important role in cloud formation.[32-34]

III. Results and discussion

A. Neat water freezing

MD simulations of freezing of neat water in contact with an ice patch provided valuable information about timescales of this process and general behavior of the SPC/E potential model with respect to the simulation box size and used cutoff distance. These results are summarized in Table 3. Simulations with *box072* (for definition see Table 1) yielded complete freezing of the system for temperatures within 5° from the estimated melting point.[17] Observed freezing above 0° indicates the approximate nature of the previously established melting point, which might in fact be somewhat higher for the SPC/E water. Note, however, that this value can be

influenced also by system size and potential cutoff distance. For lower temperatures, freezing was only partial during the 80 ns simulation. The reason for this behavior is that for low temperatures the system can get kinetically trapped in a metastable glass-like state. For the *box144* simulations, the freezing times are comparable to the previous case, however, complete freezing could be observed even for -10°. The latter system has initially a relatively smaller portion of the unit cell in the liquid phase than the former, which might turn favorable for overcoming the kinetic barriers during freezing.

For the *box360* system, complete freezing was observed only for the simulation at -5° (see Table 3 and Figure 2A). Melting occurred for all runs with temperature above the melting point, indicating that the melting temperature has somewhat decreased compared to the *box144* system. This is most likely due to the small increase of the cutoff distance.

In both *box144* and *box360* simulation cells half of the volume is initially in the solid (ice) phase. In order to investigate the influence of periodicity and the width of the ice path, we created a system of the same total size as *box360*, however, with a significantly reduced width of the initial portion in the ice phase (i.e., four oxygen bilayers in the z-direction). In this system, ice initially occupies only one quarter of the unit cell. The resulting system is denoted as *box180*. As can be seen from the Table 1, this system melts for all but one temperature (-15°), where it takes roughly 300 ns to completely freeze the whole unit cell (Fig. 2B). For the simulations where meling occurred it took considerable time to melt the ice at low temperatures, where interfaces tend to be kinetically stable and do not change for almost the whole simulation (see Fig. 2C, for example). It is worth mentioning that the initial structure should have four double-peaks in the density profile. The density profiles for the initial phase production runs have, however, only three well developed double-peaks,

which indicates a certain degree of pre-melting of the interface.

Since we observed melting even for temperatures below the estimated 0° for the constant pressure simulations, we also attempted to start the MD runs with a constant volume for the *box180* system and temperatures from -10 to +15°. With this mixed constant volume/constant pressure procedure we aimed at avoiding the effect of the pre-melting (and possible destruction of the ice part of the unit cell) by allowing for new ice to form at the interface before switching to constant pressure. Temperatures above -10° led again to ice melting, however, on a much longer time scale. The production run at -10° showed partial freezing at constant volume, so after 150 ns we switched switched to a constant pressure scheme. The change in the density profile (Figure 2D, ~150 ns) shows the consequent immediate pre-melting of the interface. An already frozen part of the interface melted and it took another 100 ns for the freezing process to start again. The system than completely froze after 500 ns of a total simulation time.

Figure 3 shows snapshots from the standard, constant pressure simulation of system *box180* 15° below the melting point. Note the gradual build up of the solid ice phase in the unit cell with increasing time. The last snapshot at 350 ns already corresponds to a completely frozen sample (in Table 3 we report a freezing time of 315 ns). According to the density profiles, the unit cell has indeed an ice phase character after 315 ns. However, to completely satisfy the ice rules, some very slow water rearrangement on a time scale exceeding the present simulations have to take place in the region where the two freezing fronts meet (Figure 3D).

The principal aim of these numerous simulations and analysis thereof was to obtain a detailed understanding of the *in silico* water freezing/melting processes and to establish a robust and reliable simulation protocol. We have obtained a general microscopic (molecular) picture of neat water freezing, melting, and premelting, the

details of which (e.g., exact melting temperature and freezing/melting timescales) can, however, depend on the particular choice of water force field.

B. Salt solution freezing

Calculations of neat water freezing were followed by simulations of brine rejection from freezing aqueous salt solutions. To this end, varying amounts of sodium and chloride ions were added to the liquid part of the simulation cell (for detailed definitions of the investigated systems see Table 2). The principal results are summarized in Table 4.

The first thing to note is that the time needed to freeze the salt containing systems generally increased compared to that for neat water (compare Table 4 with Table 3). This is a microscopic demonstration of the kinetic anti-freeze effect of the added salt. E.g., for the system with the small ice template (built from *box180*), freezing was observed only for the lowest studied temperature (-15°) and it took 350 ns (625 ns) for the systems with two (four) NaCl ion pairs to freeze, while the corresponding neat water cell froze in 315 ns. Within the present temperature grid we have seen little effect of salt on the freezing temperature. For the present low salt content the depression of the freezing temperature is expected to be small and it would probably be computationally very tedious to capture it quantitatively. The problem for more concentrated salt solutions is that we were not able to freeze ice out of them within a reasonable computer time.

Similarly to the neat water systems, under initial constant volume conditions it is possible to observe freezing also for slightly higher temperatures (Table 4). The *box180* cell with two NaCl ion pairs freezes within a time comparable to that for the constant pressure simulation (see Figure 4A for the time evolution of the density profile at -10°). In the case of the same cell with four ion pairs, the only simulation

that provided full freezing was that performed at -10° (Figure 4B). However, the time needed to fully freeze the sample was very long (810 ns). Snapshots from the course of this simulation are given in Figure 5. We clearly see from Figures 4 and 5 the process of salt rejection into the unfrozen remainder of the system. Only occasionally can an ion get trapped in the ice phase, such as one of the chlorides in Figure 5D.

In the case of systems with a larger ice template (*box360*) the effect of salt on the freezing process is even more profound (see Figures 4C and 4D). Freezing of systems with 5 NaCl ion pairs takes approximately 6-8 times longer than in case of analogous neat water cells. In this case we did not observe any problems with the initial premelting of the ice part of the cell, since this ice patch is initially large enough not to melt even at temperature close to 0°. For this reason, we were able to observeat least partial freezing up to -5°.

To characterize the hydrogen bonding network in ice and liquid water we analyzed the number of donor hydrogen bonds per each water molecule. A hydrogen bond was defined geometrically as an arrangement where the distance between the water oxygen and the second heavy atom (another water oxygen or chloride) was smaller than 3.5 Å and the angle (H-O-X, X = O or Cl^-) was smaller than 30°. In ice with a perfect tetrahedral hydrogen bonding arrangement this number should be two, each water molecule donating two and accepting two hydrogen bonds. In the liquid part of the cell we find that approximately 1.8 donor hydrogen bonds per water molecule are formed. The results of this hydrogen bond analysis for the simulation depicted in Figure 5 are displayed in Figure 6. In the ice part of the system, the number of donor hydrogen bonds to other water molecules (dashed line) is two per water molecule, whereas in the liquid part this value slightly drops, as discussed above. In the vicinity of chloride ions, the number of water-water hydrogen bonds is further decreased, while water-chloride hydrogen bonds appear. When these are

numbers are added up (solid line in Figure 6D) they show an almost perfect tetra-coordination of each water molecule even in the uncompletely frozen brine part of the cell.

IV. Summary and conclusions

We have presented results of extensive molecular dynamics simulations of freezing of neat water and aqueous sodium chloride solutions in contact with an ice patch. The freezing and salt rejection processes are analysed at a molecular detail in terms of the time evolution of the density profiles and hydrogen bonding patterns, and a robust simulation protocol within the employed force field is established. Addition of salt slows down the water freezing process, which occurs for the SPC/E model and employed ~4 nm cell size at the sub-microsecond time scale.

In the future, it will be interesting to establish how the quantitive results of the simulations, such as freezing/melting points, freezing times, salt effects, etc. depend on the particular choice of water potential.[18,35]

Acknowledgement

We are grateful to Victoria Buch for providing us with a code for generation of ice lattices and to Igal Szleifer for valuable comments. Support from the Czech Ministry of Education (Grant LC512) and the US-NSF (Grants CHE 0431312 and 0202719) is gratefully acknowledged. L.V. would like to thank the the Granting Agency of the Czech Republic (Grant 203/05/H001) for financial support and the *META*Center project for continuous computational support.

Tables:

Simulation cell code	Building block		Simulation cell properties			
	water molecules	approximate dimensions x y z / Å	construction scheme	total number of water molecules	approximate dimensions x y z / Å	cutoff distance Å
box072	72	13 x 15 x 10	S-L-L	216	13 x 15 x 32	6
box144	144	13 x 15 x 21	S-L	288	13 x 15 x 42	6
box180	180	22 x 23 x 11	S-L-L-L	720	22 x 23 x 43	9
box360	360	22 x 23 x 22	S-L	720	22 x 23 x 43	9

Table 1 Properties of the simulation cells with water/ice interfaces

simulation cell code	ice/water interface	number of NaCl ion pairs	approximate concentration
box180s02	box180	2	0.15 M
box180s04	box180	4	0.3 M
box360s01	box360	1	0.07 M
box360s02	box360	2	0.15 M
box360s05	box360	5	0.4 M

Table 2 Properties of the simulation cells with salt water/ice interfaces

relative temp.	box072		box144		box360		box180		box180 volume	
	time / ns	status	time / ns	status	time / ns	status	time / ns	status	time / ns	status
-15	80	PF	100	PF	70	PF	315	F	-	-
-10	80	PF	75	F	90	PF	110	M	500	F
-5	80	F	85	F	60	F	60	M	180	M
0	65	F	75	F	80	PF	35	M	55	M
5	55	F	25	F	50	M	2	M	4	M
10	7	M	30	M	7	M	1	M	2	M
15	13	M	15	M	3	M	<1	M	2	M

Table 3 Neat water freezing results (PF=partially frozen, F=frozen, M=melted).

relative temp.	box180s02		box180s04		box360s01		box360s02		box360s05	
	time / ns	status	time	time	time	status	time	status	time	status
-15	350	F	625	F	215	PF	310	F	560	F
-10	30 (375)	M (F)	19 (810)	M (F)	210	F	380	F	620	F
-5	10 (310)	M (F)	26 (95)	M (M)	215	F	155	F	1200	PF
0	5 (10)	M (M)	6 (75)	M (M)	205	M	620	M	65	M
5	2	M	6	M	20	M	38	M	52	M
10	1	M	<1	M	5	M	8	M	10	M
15	2	M	<1	M	3	M	4	M	3	M

Table 4 Salt water freezing results (PF=partially frozen, F=frozen, M=melted). Values in parentheses are coming from simulations employing constant pressure conditions.

Figure captions:

Figure 1: Simulation cell and corresponding oxygen density profile for *box180*. The unit cell is periodically repeated in all three dimensions.

Figure 2: Time evolution of the density profiles for neat water simulations. A) *box360* at -5 ° B) *box180* at -15° C) *box180* at -5° D*) box180* at -10° (combined constant volume/constant pressure simulation). Note the partial melting after the switch to constant pressure around 150 ns.

Figure 3: Snapshots from the simulation of the *box180* system at -15°. A) 1 ns, B) 100 ns, C) 200 ns, and D) 350 ns.

Figure 4: Time evolution of the density profiles for salt water freezing simulations. Trajectories of Na^+ and Cl^- ions are displayed as black lines. Temperature was held at -10° in all cases. A) *box180* with two NaCl ion pairs, B) *box180* with four ion pairs, C) *box360* with two ion pairs, and D) *box360* with five ion pairs.

Figure 5: Snapshots from the *box180* constant volume simulation with four NaCl ion pairs at -10°. Na^+ and Cl^- are given as light and dark spheres, respectively. A) 200 ns, B) 400 ns, C) 600 ns, and D) 815 ns.

Figure 6: Numbers of donor hydrogen bonds per water molecules for the simulation depicted in Figure 5. The plots are 1 ns averages taken at A) 200 ns, B) 400 ns, C) 600 ns, and D) 815 ns. Water-water and water-chloride hydrogen bonds are given as dashed and dotted lines, respectively. Solid line gives the total number of donor hydrogen bonds that a water molecule forms.

Figure 1:

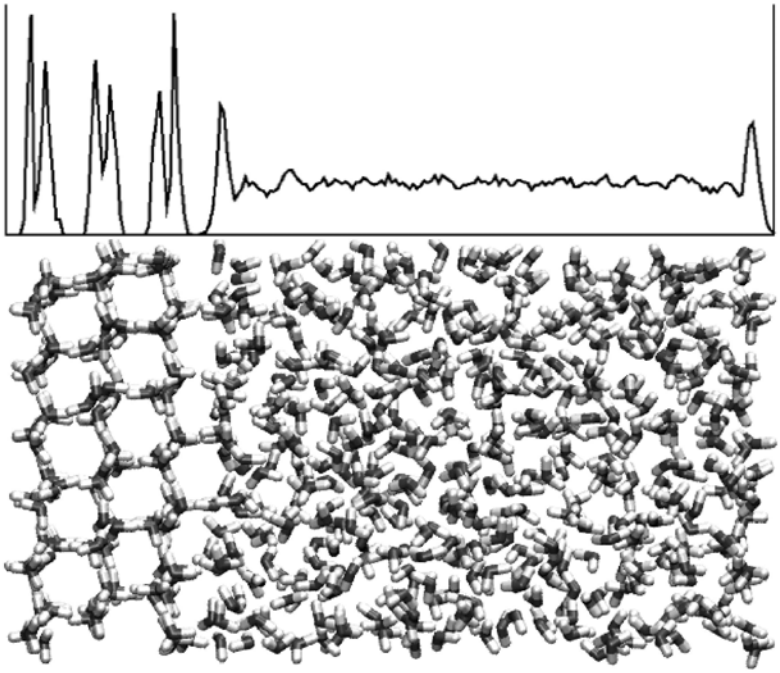

Figure 2:

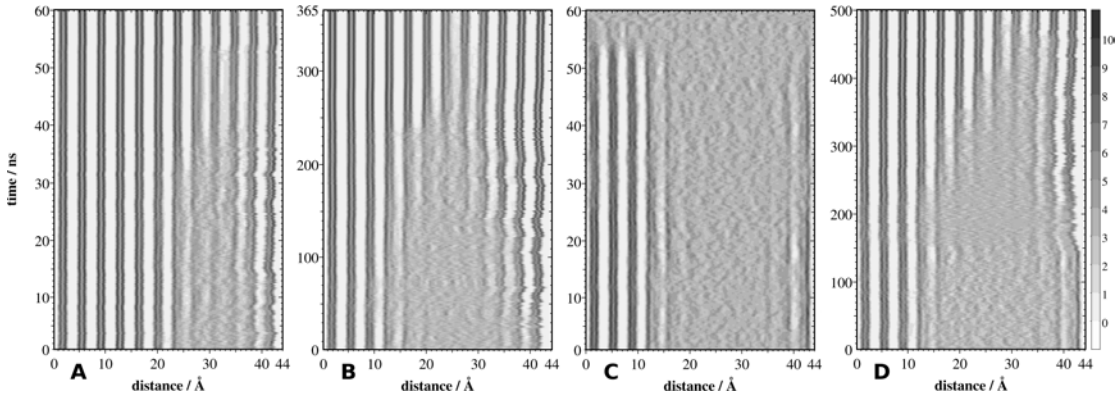

Figure 3:

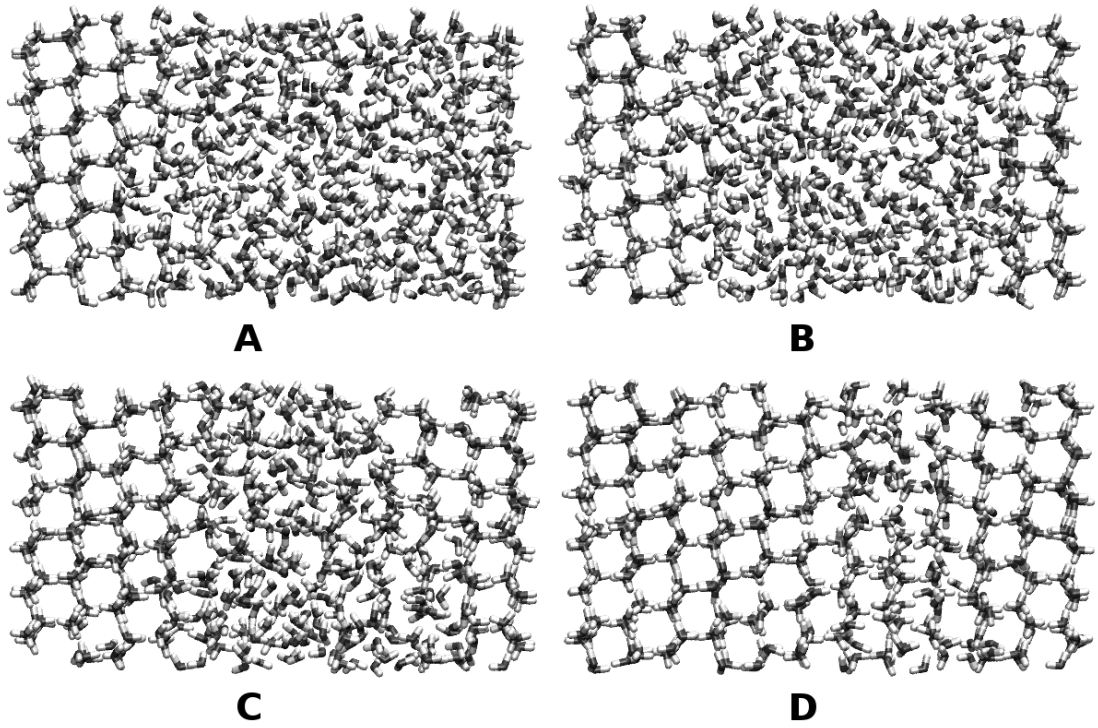

Figure 4:

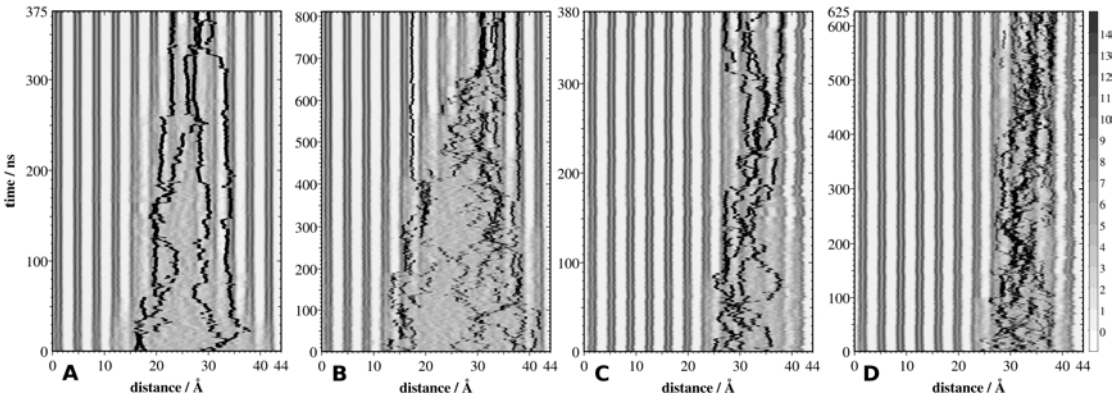

Figure 5:

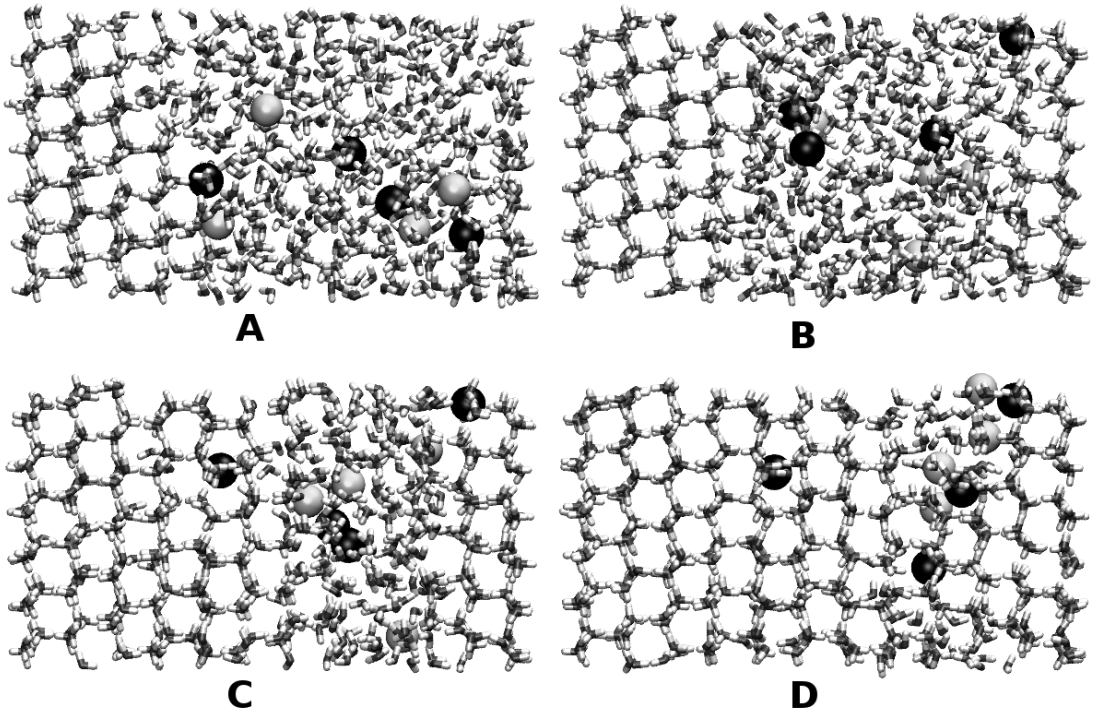

Figure 6:

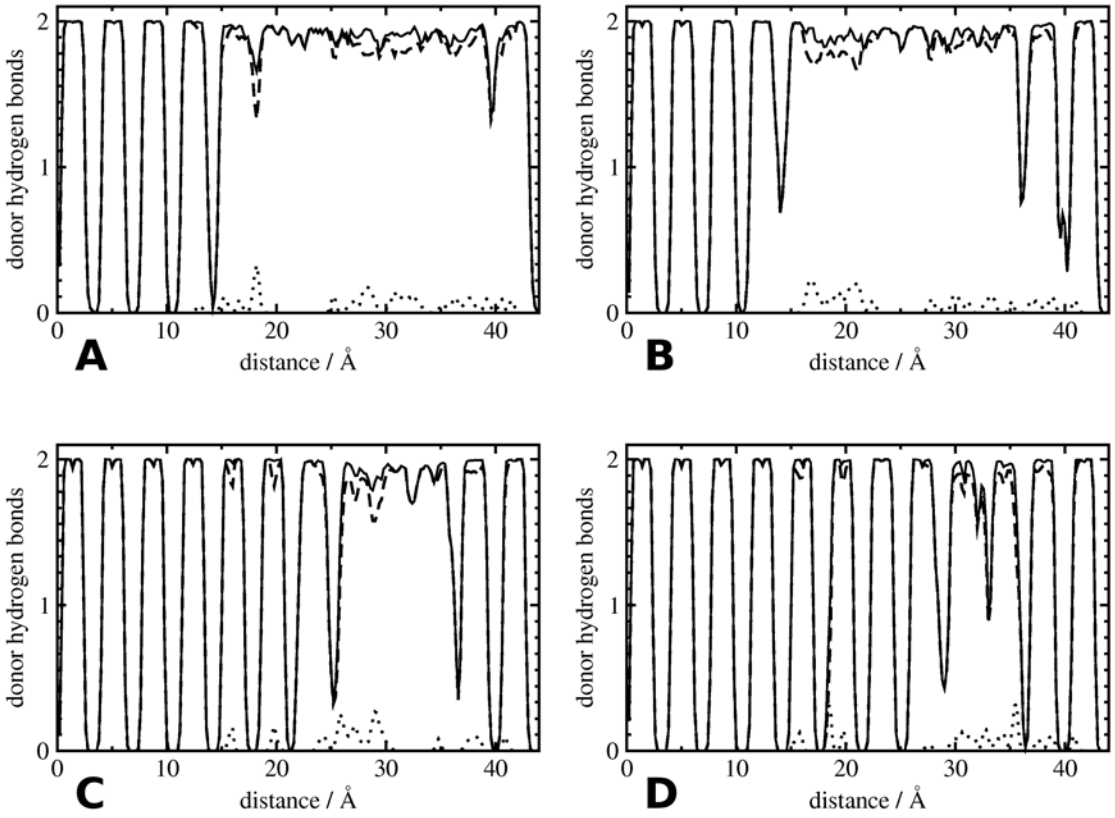

References:

(1) Matsumoto, M.; Saito, S.; Ohmine, I. *Nature* **2002**, *416*, 409.

(2) Wales, D. J.; Doye, J. P. K.; Miller, M. A.; Mortenson, P. N.; Walsh, T. R. Energy landscapes: From clusters to biomolecules. In *Advances in Chemical Physics, Volume 115*, 2000; Vol. 115; pp 1.

(3) Mucha, M.; Jungwirth, P. *Journal of Physical Chemistry B* **2003**, *107*, 8271.

(4) Karim, O. A.; Haymet, A. D. J. *Chemical Physics Letters* **1987**, *138*, 531.

(5) Karim, O. A.; Haymet, A. D. J. *Journal of Chemical Physics* **1988**, *89*, 6889.

(6) Laird, B. B.; Haymet, A. D. J. *Chemical Reviews* **1992**, *92*, 1819.

(7) Hayward, J. A.; Haymet, A. D. J. *Journal of Chemical Physics* **2001**, *114*, 3713.

(8) Hayward, J. A.; Haymet, A. D. J. *Physical Chemistry Chemical Physics* **2002**, *4*, 3712.

(9) Bryk, T.; Haymet, A. D. J. *Molecular Simulation* **2004**, *30*, 131.

(10) Nada, H.; Furukawa, Y. *Journal of Crystal Growth* **2005**, *283*, 242.

(11) Nada, H.; van der Eerden, J. P.; Furukawa, Y. *Journal of Crystal Growth* **2004**, *266*, 297.

(12) Yamada, M.; Mossa, S.; Stanley, H. E.; Sciortino, F. *Physical Review Letters* **2002**, *88*.

(13) Nada, H.; Furukawa, Y. *Journal of Physical Chemistry B* **1997**, *101*, 6163.

(14) Svishchev, I. M.; Kusalik, P. G. *Journal of the American Chemical Society* **1996**, *118*, 649.

(15) Carignano, M. A.; Shepson, P. B.; Szleifer, I. *Molecular Physics* **2005**, *103*, 2957.

(16) Berendsen, H. J. C.; Grigera, J. R.; Straatsma, T. P. *Journal of Physical Chemistry* **1987**, *91*, 6269.

(17) Vega, C.; Sanz, E.; Abascal, J. L. F. *Journal of Chemical Physics* **2005**, *122*.

(18) Nada, H.; van der Eerden, J. *Journal of Chemical Physics* **2003**, *118*, 7401.

(19) Vrbka, L.; Jungwirth, P. *Physical Review Letters* **2005**, *95*, 148501.

(20) Shcherbina, A. Y.; Talley, L. D.; Rudnick, D. L. *Science* **2003**, *302*, 1952.

(21) Aagaard, K.; Carmack, E. C. *Journal of Geophysical Research-Oceans* **1989**, *94*, 14485.

(22) Jungwirth, P.; Rosenfeld, D.; Buch, V. *Atmospheric Research* **2005**, *76*, 190.

(23) Essmann, U.; Perera, L.; Berkowitz, M. L.; Darden, T.; Lee, H.; Pedersen, L. G. *Journal of Chemical Physics* **1995**, *103*, 8577.

(24) Ryckaert, J.-P.; Ciccotti, G.; Berendsen, H. J. C. *Journal of Computational Physics* **1977**, *23*, 327.

(25) Berendsen, H. J. C.; Postma, J. P. M.; Vangunsteren, W. F.; Dinola, A.; Haak, J. R. *Journal of Chemical Physics* **1984**, *81*, 3684.

(26) Duke, R. E.; Pedersen, L. G. Pmemd 3; University of North Carolina: Chapel Hill, 2003.

(27) Case, D. A. P., D.A.; Caldwell, J.W.; Cheatham III, T.E.; Wang, J.; Ross, W.S.; Simmerling, C.L.; Darden, T.A.; Merz, K.M.; Stanton, R.V.; Cheng, A.L.; Vincent, J.J.; Crowley, M.; Tsui,V.; Gohlke, H.; Radmer, R.J.; Duan, Y.; Pitera, J.; Massova, I.; Seibel, G.L.; Singh, U.C.; Weiner, P.K.; Kollman, P.A. Amber 7; University of California: San Francisco, 2002.

(28) Smith, D. E.; Dang, L. X. *Journal of Chemical Physics* **1994**, *100*, 3757.

(29) Buch, V.; Sandler, P.; Sadlej, J. *Journal of Physical Chemistry B* **1998**, *102*, 8641.

(30) Johari, G. P. *Journal of Chemical Physics* **2005**, *122*.

(31) Morishige, K.; Uematsu, H. *Journal of Chemical Physics* **2005**, *122*.

(32) Whalley, E. *Journal of Physical Chemistry* **1983**, *87*, 4174.

(33) Whalley, E. *Science* **1981**, *211*, 389.

(34) Murray, B. J.; Knopf, D. A.; Bertram, A. K. *Nature* **2005**, *434*, 202.

(35) Horn, H. W.; Swope, W. C.; Pitera, J. W.; Madura, J. D.; Dick, T. J.; Hura, G. L.; Head-Gordon, T. *Journal of Chemical Physics* **2004**, *120*, 9665.